Journal of Industrial and Engineering Chemistry 83 (2020) 323–332

Contents lists available at ScienceDirect

Journal of Industrial and Engineering Chemistry

journal homepage: www.elsevier.com/locate/jiec

Biofabrication and application of decellularized bone extracellular matrix for effective bone regeneration

Min Suk Lee[a,b], Dong Hyun Lee[a], Jin Jeon[a,b], Giyoong Tae[c], Young Min Shin[a,b,*], Hee Seok Yang[a,b,*]

[a] Department of Nanobiomedical Science & BK21 PLUS NBM Global Research Center for Regenerative Medicine, Dankook University, Cheonan, 31116, Republic of Korea
[b] Center for Bio-Medical Engineering Core-Facility, Dankook University, Cheonan, 31116, Republic of Korea
[c] School of Materials Science and Engineering, Gwangju Institute of Science and Technology, 123 Cheomdan-gwagiro, Buk-gu, Gwangju, 61005, Republic of Korea

ARTICLE INFO

Article history:
Received 24 October 2019
Received in revised form 26 November 2019
Accepted 5 December 2019
Available online 16 December 2019

Keywords:
Bone powder
Demineralized bone matrix
Decellularization
Bone tissue engineering
Mouse calvarial defect model

ABSTRACT

In order to promote effective healing of a bone defect, various bone grafts have been widely implanted into defect sites. However, several drawbacks, such as immunologic rejection, insufficient tissue healing, or secondary damage to the donor site, are still concerns. These limitations of the current bone grafts can be overcome by use of a natural ECM that can influence basic cellular behaviors, such as proliferation, migration, and differentiation. Herein, we introduce a novel bone decellularized ECM (bdECM) material extracted from bovine bones via demineralization and decellularization. This sequential process enabled us to prepare raw material possessing higher contents of native BMP-2 and BMP-7, and a fibrous microarchitecture resembling the collagen bundle in the ECM was maintained. Furthermore, residual calcium and phosphate originated from the bovine bone were considerably removed, and contamination by residual DNA was significantly reduced during the fabrication process. These features enabled the scaffold successfully promote mineralization of the cultured primary osteoblasts *in vitro*, which was significantly better than those from the bone powder or demineralized bone matrix. In a mouse calvarial defect, new bone formation was improved in the bdECM group and the density of those was also higher than other groups.

Introduction

Bone fractures resulting from trauma, diseases, or pathological degeneration are hard to treat effectively [1]. To treat a bone defect, an autologous bone graft has been considered to be the gold standard medication in many clinical cases [2,3]. However, an autograft can be a burden on patients with secondary surgery and may be restricted because of available donor-tissue limitations [4]. Although this drawback are now advanced by the use of various artificial bone grafts made of metals, ceramics, or synthetic polymers, their effects in promoting endogenous bone healing were not hopeful. Unfortunately, they could lead to a clinical immunogenic response [5]. Thus our eyes are focusing on a natural platform, especially the use of demineralized bone matrix (DBM)-derived from the native tissue was recognized as an alternative for those artificial bone-graft materials. It is a mineral-deficient animal-derived material produced by acidic extraction and contains a variety of proteins in bones [4,5]. Several studies have described its efficacy for osteoinduction in various animal models [6,7], and growth factors, non-collagenous proteins and type I collagen in DBM have been known to regulate the bone regeneration [4,5]. Also, there are various types of commercialized DBM available, which could be customized for target tissues [8].

Even though DBM materials have shown an advanced effect in healing the bone defect than the synthetic materials, there are still several concerns related to the safety and efficiency [9,10]. These issues may be involved the manufacturing process of DBM. For example, raw materials for DBM are fragmented in small particulates and then immersed in a hydrogen chloride (HCl) solution to remove residual inorganic components. After washing process, final product is obtained. However, this process may be insufficient to expose the fundamental structure of extracellular matrix (ECM) which could be obtained by HCl solution and it cannot allow release of entrapped growth factors in the ECM that

* Corresponding authors at: Department of Nanobiomedical Science, Dankook University, 119 Dandae-ro, Dongnam-gu, Cheonan-si, 31116 Republic of Korea.
E-mail addresses: ymshin@dankook.ac.kr (Y.M. Shin), hsyang@dankook.ac.kr (H.S. Yang).

https://doi.org/10.1016/j.jiec.2019.12.005
1226-086X/

can effectively promote the bone healing. Also, the DBM commercialized or used in a clinical field does not contain ECM-like microstructure and cannot release the growth factor remaining inside of the materials. It is clear that their effect in the bone healing may not be maximized. Furthermore, residual cellular component in the DBM can cause unexpected adverse effects, which may be involved in animal deaths or severe inflammatory reaction *in vivo*.

As widely known, a mimicry of ECM in the native tissue is one of the interesting approaches in tissue engineering [11]. The ultimate goal of this trial is to reconstruct a 3D microenvironment including both structural platform and soluble factor delivery system [11,12]. Because whole tissues in the body have consisted largely of ECM that influences the biological behavior of cells, such as cellular adhesion, proliferation, and differentiation. In fact, mimicking the complex microenvironment as like host tissue needs further advances [2]. Thus, organ decellularization is used to make an ECM-rich microenvironment as another option [12]. ECM derived from specific tissues using decellularization still holds various ECM proteins, such as type I collagen, laminin, fibronectin, and growth factors, in its entirety [4,11,13,14]. Previously reports have described that specific tissue or organ derived ECM can preserve proper phenotype in *in vitro* culture system, improve differentiation of progenitor cells at relevant tissue site. These results might be caused that specific tissue or organ derived ECM provide tissue-specific signals which is contained physiological relevance and specific biochemical profiles [14]. In addition, manufacturing process for decellularized ECM can make them safe to be used as a scaffold by removing nuclear components and cell membrane antigens, and thus minimize the immune response [15]. These facts inspired us to find an alternative platform for bone regeneration that was safe and much more osteoinductive than DBM.

In this study, we extracted a novel bone graft substitute, native bone decellularized ECM (bdECM) from bovine bone via demineralization and decellularization processes. This sequential process allows removal of inorganic components from the bone as well as exposure of ECM structure while maintaining higher contents of soluble factors. Also, the bdECM was removed residual DNA via decellularization process that ensure the safety issue different from the DBM. We hypothesized that bdECM components including structural proteins and bioactive growth factors would improve bone regeneration by providing those unique tissue-specific signals to host cells at the defect sites better than bone powder and DBM. We confirmed the morphological differences and whether they included calcium and phosphate by means of surface analyses that compared bdECM and others. To investigate the extent of decellularization, the bdECM was stained nucleus and quantified with DNA. We examined the bdECM and others to see if they could provide natural growth factors, such as bone morphogenetic protein 2 and 7 (BMP-2 and BMP-7), to specifically affect promote osteogenesis. Also, we evaluated whether bdECM and other groups could induce mineralization of primary isolated osteoblasts via *in vitro* osteogenic differentiation. Furthermore, we did an *in vivo* animal study using a mouse calvarial defect model for eight weeks. We used a live micro-computed tomography (micro-CT) and histological analysis to compare tissue compatibility and bone formation between the bdECM and other groups.

Material and methods

Preparation of bone decellularized extracellular matrix

We purchased fresh bovine femurs from cattle aged 24 months from a qualified butcher shop (Farm Story Hannaeng, Cheongju, Korea) and received them in segmented tube form (Fig. 1). The segmented bones were stored at −20 °C to maintaining osteoinductive potential. Before we did the demineralization step, bones were washed in 6 % hydrogen peroxide solution for three days to remove lipids and some debris. The bones were then vacuum-dried (OV-11, Jeio Tech, Daejeon, Korea) for one day. The dried bones were immersed in liquid nitrogen, crushed, and ground to fabricate

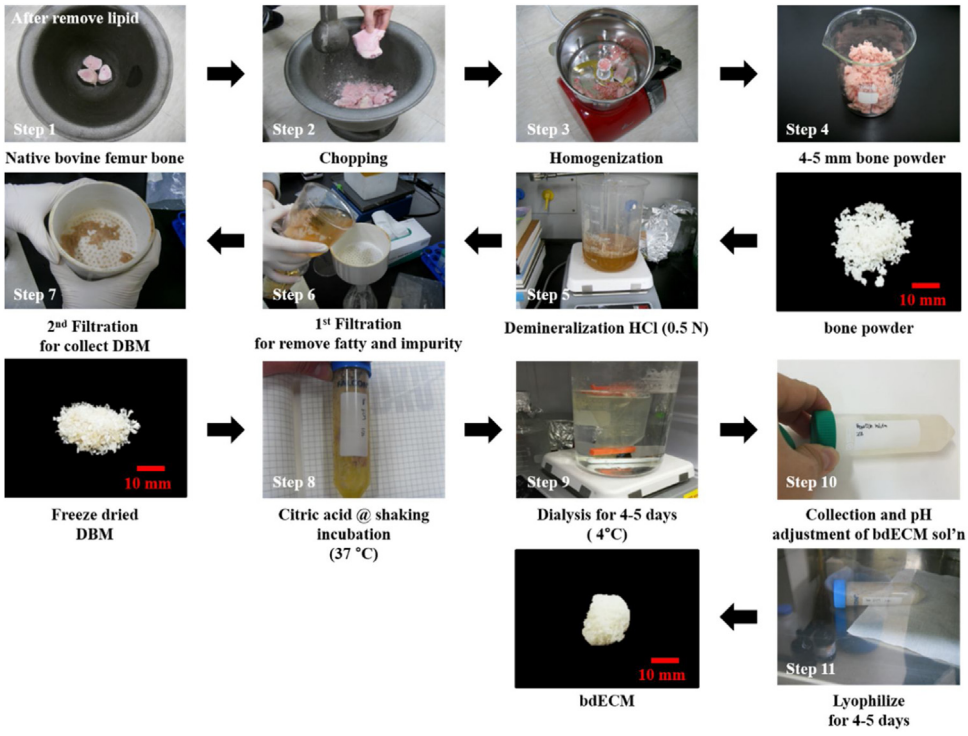

Fig. 1. Representative macroscopic images of fabrication procedure about bdECM.

proper sizes which were $4 \times 4 \times 4\,mm^3$ or less for bone powder. The bone fragments were immersed in 0.5 N hydrogen chloride to demineralize the calcium, phosphate, and other inorganic substances for three days. The demineralized bone fragments were rinsed using 70 % ethanol overnight. The rinsed bone fragments were frozen, lyophilized overnight, and were then referred to as demineralized bone matrix (DBM). In the decellularization step, DBMs were soaked in 0.6 N citric acid to decellularize them for three days, and dialyzed in distilled water to reach *p*H 7.0. The resultant material, referred to as bdECM, was rinsed in phosphate-buffered saline (PBS, Sigma-Aldrich) supplemented with 1 % w/v penicillin/streptomycin (Sigma-Aldrich) under continuous agitation overnight at 4 °C to remove residual cellular material. The bdECM was then snap frozen, lyophilized overnight, and stored at −20 °C until required. To confirm nuclei stain, bone powder, DBM, and bdECM were embedded in an optimal cutting-temperature compound at−20 °C, sectioned into 12-μm thick slices, and stained with 4′,6-diamidino-2-phenylindole (DAPI, DAPI-Vectashield, Vector Laboratories, Burlingame, CA, USA). Optical (CKX41, Olympus, Tokyo, Japan) and fluorescence microscopes (IX71 inverted microscope; Olympus, Tokyo, Japan) were used to obtain images of the stained samples for confirming the stained nuclei.

Morphology and surface characteristics

The morphologies of bone powder, DBM, and bdECM were investigated via macroscopy and a scanning electron microscope (SEM, JSM-6510, JEOL Co., Tokyo, Japan). All bone powder, DBM, and bdECM were sputter-coated (Sputter Coater 108 Auto, Cressington, Watford, UK) with platinum for 180 s prior to SEM measurements. The crystallographic properties of the bone powder, DBM, and bdECM were investigated by X-ray diffraction (XRD, Ultima IV, Rigaku, Tokyo, Japan) measurement. The XRD was activated at 40 kV and 40 mA with Cu Kα1 radiation (λ = 1.5405 Å). The patterns of XRD were measured at a step-scan of 0.02° and rate of 3° per minute over a 2θ range from 20 to 80°. The surface atomic compositions of bone powder, DBM, and bdECM were measured using X-ray photoelectron spectroscopy (XPS, Escalab 220i-XL, VG Scientific Instruments, East Grinstead, UK) at base pressures < 10−10 mbar. The photoelectron spectra were excited using an Al Kα (1486.6 eV) anode at a constant power of 100 W (15 KV and 10 mA).

Assessment of cellular contents

We quantified the DNA contents by adapting previously reported methods [16,17]. Bone powder, DBM, and bdECM were digested using pepsin (1 mg/mL) in HCl solution (0.01 M) and centrifuged at 2,980 g for 10 min to remove protein remains. The supernatants were then centrifuged in phenol/chloroform/isoamyl alcohol (25:24:1, Sigma-Aldrich) at 10,000 g for 30 min. The DNA was precipitated from the aqueous phase using a 3 M sodium acetate/ethanol solution (v/v = 1:20) at −20 °C overnight. The extracted DNA samples were then dehydrated in a vacuum oven at room temperature and rehydrated in 1x Tris-EDTA buffer (Sigma-Aldrich). Finally, the concentration of each extracted DNA sample was measured using a Nanodrop (NanoDrop One, Thermo Fisher Scientific).

Quantification of BMP-2 and BMP-7 on bone powder, DBM, and bdECM

For the quantification of BMP-2 and BMP-7, bone powder, DBM, and bdECM of 10 mg were homogenized in 1 mL of PBS on ice. The homogenized samples were sonicated for 5 min and centrifuged for 5 min at 5000 g. Next, the supernatants were removed and the remaining samples were analyzed by using ELISA kits for BMP-2 (SEA013Bo, Cloud-Clone Corp., TX, USA) and BMP-7 (E0254Bo, Bioassay Technology Laboratory, Shanghai, China) according to the manufacturer's protocol.

In vitro Osteogenic differentiation test

We obtained primary isolated rat osteoblasts from the calvaria of a neonatal rat (1–2 days old) and cultured them in growth medium, which was Dulbecco's modified Eagle's medium (DMEM, Corning, NY, USA) supplemented with 10 % fetal bovine serum (FBS, Corning, NY, USA) and 1 % penicillin / streptomycin until they were confluent. When the osteoblasts were proliferated confluence, the media were changed to an osteogenic medium, which was added to dexamethasone (Sigma-Aldrich) of 100 nM, L-ascorbic acid (Sigma-Aldrich) of 50 μM, β-glycerophosphate (Sigma-Aldrich) of 10 mM, and L-glutamine (Sigma-Aldrich) of 7 mM in the growth medium, and 1 mg of each sample of bone powder, DBM, and bdECM was placed in Transwell® inserts (Corning, NY, USA). The osteoblasts were cultured with materials indirectly for two or four weeks, and the osteogenic medium was changed to fresh medium every two days. After two or four weeks, cultured osteoblasts were fixed with 4 % paraformaldehyde (Sigma-Aldrich) for 15 min and washed twice with PBS. The washed cells were stained with 2 % Alizarin red S (Sigma-Aldrich) for 15 min or 5 % silver nitride (Sigma-Aldrich) under UV radiation for 30 min.

To evaluate the osteogenic-related gene expression, we isolated RNA from cells at two and four weeks after differentiation using the TRIzol reagent (Ambion) following the manufacturer protocol. The RNA was quantified by absorbance readings at 260 nm and 280 nm using nanodrop. The RNA was purified, and we synthesized the first-strand cDNA from 1 ug of total RNA using Accupower RT-PCR premix (Bioneer). Synthesized cDNA was used as a template for amplification of RUNX2, osteopontin (OPN), osteocalcin (OCN), and GAPDH in PCR reactions containing Accupower PCR premix (Bioneer) and the primers (Table 1). PCR products were resolved by agarose gel electrophoresis.

In vivo animal test

The female ICR mice (six weeks old, Dayun, Gyeonggi-do, Korea) were given an intraperitoneal injection of 2 % avertin (20 μL / g mouse body weight). In the mice, we made a longitudinal incision in the midline of the cranium from the nasal bone to the posterior nuchal line. The incised skin was spread to expose the surface of these parietal bones. We prepared two circular transosseous defects of 4 mm in the mouse skulls using a surgical trephine burr (Ace Surgical Supply Co., Brockton, MA, USA) which was maintained by a low-speed micromotor. The defect site was frequently cooled down with sterilized PBS to prevent tissue damage. Five animals (10 defects) were used in each group. The bone powder, DBM, and bdECM of 1 mg were implanted into each defect site (n = 10). The mice were sacrificed after eight weeks and

Table 1
RT-PCR primer sequence for osteogenic genes.

Gene	Primers	Annealing Temperature (°C)
RUNX2	5′-GAACTGATAGGACGCTGACG-3′ 5′-GCTTCTCCAACCCACGAATG-3′	55 °C
OCN	5′-AGCTCAACCCCAATTGTAGC-3′ 5′-AGCTGTGCCGTCCATACTTT-3′	55 °C
OPN	5′-TGAAACTCGTGGCTCTGATG-3′ 5′-GATGAACCAAGCGTGGAAAC-3′	55 °C
GAPDH	5′-GCCATGAGGTCCACCACCCT-3′ 5′-AAGGTCATCCCAGAGCTG-3′	60 °C

harvested to be fixed in a 4 % paraformaldehyde solution. The animal study was approved by the Institutional Animal Care and Use Committee at Dankook University (DKU-16-005).

Micro-CT analysis

At 2, 4, 6, and 8 weeks, we anesthetized the mice in each group in the same way and did live micro-CT scans (Skyscan 1172, Skyscan, Kontich, Belgium) to analyze new bone formation and bone density. Micro-CT was set at 50 kV, 500 μA, aluminum filter of 0.2 mm and we scanned all specimens. After eight weeks, all mice of groups were sacrificed, harvested, and analyzed. Scanned images were reconstructed by using the Skyscan NRecon program. The Skyscan Dataviewer program presented color meter which is indicated tissue density that is possible to compare density within each sample, not group. Following reconstruction, the images in the region of interest were set up to operate Skyscan CTan and CTvol programs in order to visualize and quantify the bone volume per tissue volume (BV/TV) and bone mineral density (BMD). In Bone powder group, we scanned mouse immediately after implantation for getting initial results of bone volume and density (Day 0). After 8 weeks, we quantified the bone volume and density after deducting the value of Day 0.

Histological analysis

After eight weeks, we fixed the retrieved mouse calvarial tissues with paraformaldehyde (PFA, Sigma-Aldrich), rinsed with PBS for removing residual PFA, immersed in Decalcifying Solution-Lite (Sigma-Aldrich) at room temperature for 6 h. Next the samples were dehydrated with a graded ethanol series and embedded in paraffin. The samples were sectioned with a thickness of 6 μm by a microtome (RM2255, Leica, Bensheim, Germany). Sectioned samples were deparaffinized in xylene, hydrated with a series of graded ethanol, and stained with hematoxylin & eosin (H&E) and Goldner's trichrome staining. We used an optical microscope to obtain images of the stained samples for confirming the deposition of mineralization in all groups. The visualized bone-regeneration area was quantified as percentage ratios of regenerated bone formation and bone density using Image J software (National Institutes of Health, Bethesda, MD, USA) with the following equation.

$$\textbf{New bone formation area} = \left(\frac{\textbf{New bone area}}{\textbf{Bone defect area}}\right) \times 100$$

$$\textbf{Bone density} = \frac{\textbf{New bone area}}{\textbf{New bone area} + \textbf{Fibrovascular tissue area}} \times 100$$

Immunohistochemical analysis

In order to confirm the expression level of osteopontin (OPN), we randomly selected paraffin sectioned slides ($n = 3$ sectioned slide/samples of each group) and immersed them in xylene for deparaffinization. Then samples were hydrated for the preconditioned process to be stained and incubated using blocking buffer solution, which contained 10 % horse serum and 0.5 % Triton X-100 in PBS at room temperature. The blocked samples were stained with primary mouse specific antibodies, which were 1:100 diluted for OPN (Abcam) overnight at 4 °C. We used fluorescein-isothiocyanate conjugated secondary antibodies (Jackson Immuno Research Laboratories) to visualize them with OPN positive signals and counterstained them with DAPI. Immunostained samples were photographed by means of a fluorescence microscope (U-RFLT50, Olympus, Shinjuku, Japan) at the Cheonan Core Facility Center.

Statistical analysis

Quantitative data are presented as means ± standard deviation. Statistical analyses were carried out using Student's *t*-test and the Origin Pro 8 SR4 software (OriginLab Corp., MA, USA). A $p < 0.05$ was considered to indicate statistical significance.

Results and discussion

Preparation of bdECM

As described earlier, even though implantation of DBM exhibit regenerative potential in a bone healing, several issues are still

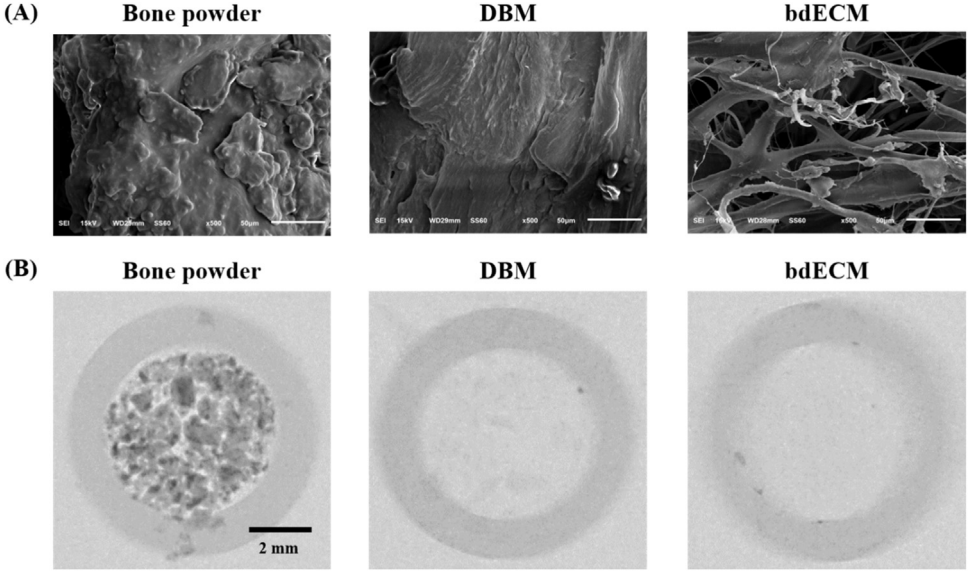

Fig. 2. Morphological characteristics and observation of remaining inorganic components. Representative (A) SEM and (B) micro-CT scan images of bone powder, DBM, and bdECM.

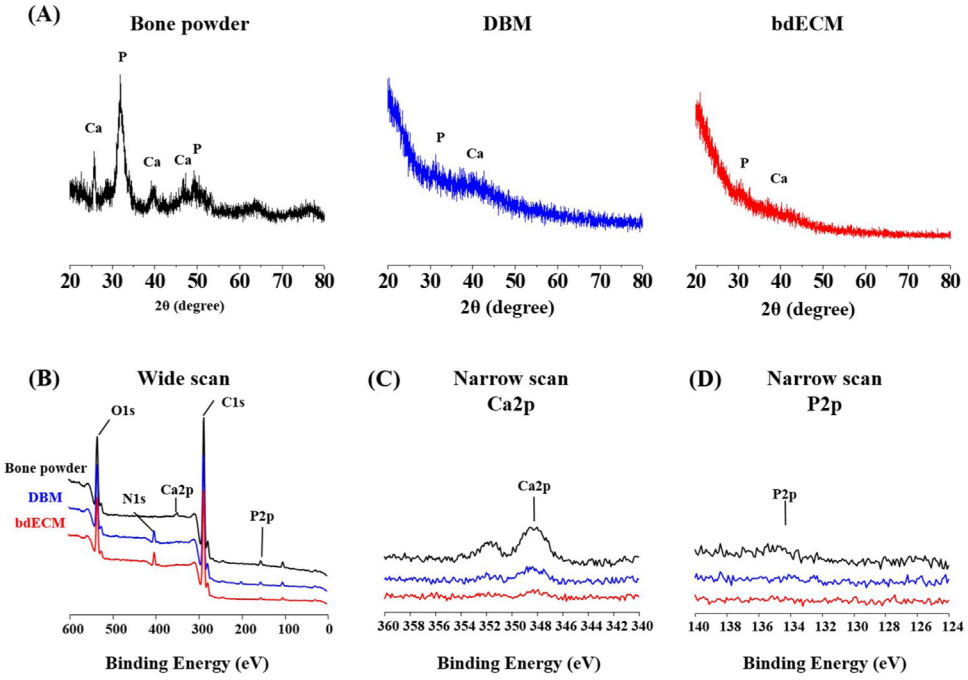

Fig. 3. Surface analyses to investigate mineral elements contained in bone powder, DBM, and bdECM. The results of (A) XRD spectra, (B) XPS wide scan, the narrow scan of (C) Ca2p and (D) P2p.

concerned. For the effective implantation and better handling, they should be delivered with various carrier molecules [4]. These platforms might be induced adverse effects because it is hard to be modeled a desire shape, maintained localization with DBM particles by degrading carrier. Other issues are residual cellular components and hiding (masking) the native ECM structure, and following inhibiting growth factor release. This occurs immune responses or being less effective in bone regeneration. In the present study, we performed demineralization process to use bovine bone for fabricating DBM and added decellularization process to extract native ECM and to avoid those problems. Additional decellularization successfully removed the residual cellular components as well as allowed to be exposed fibrous ECM structure hided in the DBM. In addition, this product well dispersed in a water or organic solvents, various form of scaffolds or hydrogel can be made.

Optimal sequential processes for demineralization and decellularization in preparing bdECM are depicted in Fig. 1. Bovine femur bone was immersed in hydrogen peroxide to remove lipids and fragmented to prepare irregular polygonal shapes of 4 mm^3 size bone powder. Inorganic elements were removed from the bone powder by acid extraction for preparation of DBM. The fabricated DBM, which still maintained irregular polygonal shapes, was digested and solubilized with citric acid to remove remaining cellular debris. After the following process, we obtained bdECM similar to soft tissue like sponge shape. The bdECM was further evaluated *in vitro* and *in vivo* experiments as a biological scaffold compared to bone powder and DBM.

Characterization of bone powder, DBM, and bdECM

Morphological changes of the specimens going through the demineralization and decellularization were verified with SEM (Fig. 2A). The bone-powder group after treatment with hydrogen peroxide still contained tissue-derived debris on the surface and looked much rougher than other groups. The DBM group relatively appeared to have a flatter surface than did bone powder; each face of polygonal shape was close to the results from previous reports [18,19]. The bdECM group exhibited clear fibrous structures with larger pores than did the others. Although both bone powder and DBM were composed of a dense collagenous matrix with small pores, they had interconnected pores inside [20,21]. The bdECM group would provide much more opportunity that host bone-forming cells would infiltrate inside by revealing a cell-adhesion motif on the fiber of bdECM.

The presence of inorganic components in the bdECM group was identified by micro-CT, XRD, and XPS analysis. As depicted in Fig. 2B, whereas several inorganic components in the bone-powder group were clearly revealed in a soft X-ray image by micro-CT, no signals were detected in the DBM and bdECM groups. In addition, the bone powder exhibited several diffraction peaks of hydroxyapatite at 2θ = 25.8 (002, Ca), 31.9 (211, P), 39.7 (310, Ca), 45.5 (203, Ca), and 47.7 (312, P) (Fig. 3A) [13,22]. The quantity of calcium and phosphate was significantly decreased in the DBM group, and much lower signals of them were detected in the bdECM group. The XPS analysis also revealed the consistency of the results for the presence of inorganics in the ECM (Fig. 3B-D and Table 2).

The bone-powder group showed calcium and phosphate contents at 0.6 % (Ca2p, 348 eV) and 0.1 % (P2p, 135 eV) rates, respectively. However, the phosphate peak was not detected in either the DBM or the bdECM group; the only small intensity of calcium contents appeared at 0.2 % and 0.1 % for each group. As the demineralization or decellularization progressed, nitrogen (N1s) contents indicating amine group (3.7 % and 4.6 % at 401 eV) newly

Table 2
XPS atomic analysis of bone powder, DBM, and bdECM.

Materials	Atomic %				
	C1s	O1s	N1s	Ca2p	P2p
Bone powder	80.5	18.8	–	0.6	0.1
DBM	78.6	17.5	3.7	0.2	–
bdECM	79.7	15.6	4.6	0.1	–

appeared in the DBM and bdECM groups, indicating that relative protein contents were increased, or a basement protein layer was exposed by removing the inorganic contents. Thus, we found that most inorganic components were removed during the demineralization.

Configuration of cellular nucleus and quantification of contained DNA and BMPs

One major issue in preparing biological scaffolds using decellularization is how to completely remove the cellular contents that can cause an immunogenic response during the fabrication process. For example, residual DNA can harm the host cells or induce an M1-type macrophage response around the host-implanted area [23,24], and an oligosaccharide molecule, galactose-α1,3-galactosyl-β,4-N-acetylglucosamine (α-Gal) epitope, which is discovered at cell surfaces in non-primate mammals, including pigs and cows, can cause an immunogenic response in the human body [4,13]. Thus, cellular contents in the decellularized scaffolds should be removed to prevent the possibility of the immune response. In previous literature, the efficacy of decellularization was defined via minimal criteria that prove the extent of the removal of nuclei and possession of double-stranded DNA of less than 50 ng per mg initial dry weight of the decellularized product [4,13,15,23,24]. Thus, we measured the residual DNA contents and visualized the presence of nuclei by staining DAPI in DBM and bdECM (Fig. 4A). In the stained results, the bdECM group was hardly stained with DAPI, whereas several nuclei were stained in the DBM group. We found that removal of cellular content was effective using decellularization. The DNA content in the bdECM group was 23.96 ± 1.53 ng/mg dry weight, which was significantly less than that in the bone powder (113.53 ± 8.92 ng/mg dry weight) and DBM (72.73 ± 0.41 ng/mg dry weight) groups (Fig. 4B). The DNA content of the bdECM group was much lower than 50 ng/mg dry weight, which was completely decellularized and satisfied the minimum standards of immune response available in medical applications [4,15,23]. Also, the decellularization step itself might remove the remaining α-Gal epitope during the process, and small amounts of the α-Gal epitope are too little to cause an adverse effect in the host [4,25]. On the other hand, DNA contents from the DBM group in our experiments were higher than those from other reports [4,13]. In preparation of DBM, we did not use the organic solvents for delipidation as a washing step after demineralization. Although demineralization can remove residual DNA sufficiently [26], it can destroy the ECM ultrastructure [23], damage structural superficial [27], and cause carcinogenesis [28]. Thus, we minimized use of a hazardous solvent for conservation of a physiologically relevant environment and ECM-incorporated growth factors in extracted bdECM.

The preserved amount of BMPs after demineralization merely lies within the nanogram range of DBM; moreover, the absolute amount of BMP per DBM product differs between various batches of the same DBM product. A number of studies using DBM have showed adverse effects that were appeared a significant reduction of mineralization in *in vitro* osteogenic differentiation test using DBM-present medium and poor bone formation and acute toxic reaction using implantation of DBM [4,9,10,29]. Herein, we determined whether our sequential process for bdECM can preserve BMPs in the material or easily release BMPs from the material. As shown in Fig. 4C, BMP-2 content in the bdECM group was 34.75 ± 2.77 pg/mg dry weight, which was significantly higher than that of the bone powder (24.04 ± 2.91 pg/mg) or DBM (25.35 ± 1.28 pg/mg) groups. Also, BMP-7 content in the bdECM (12.25 ± 0.43 ng/mg) group was higher than that in the bone powder (9.92 ± 0.20 ng/mg) or DBM (12.16 ± 0.23 ng/mg) groups (Fig. 4D). In these results, we ground bone powder and DBM to

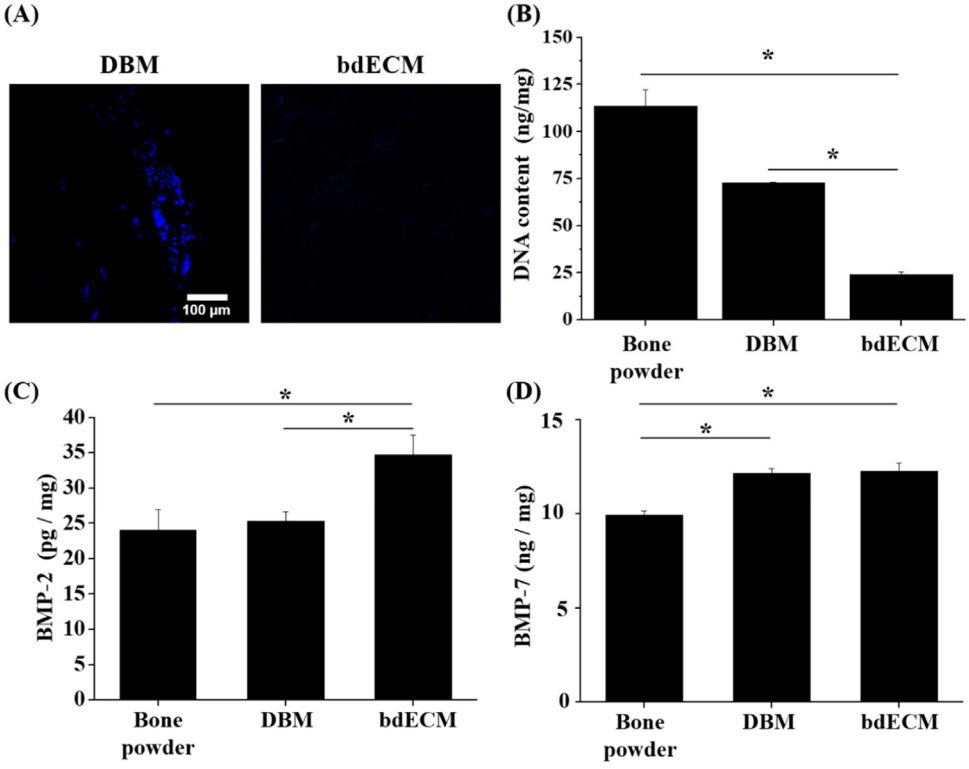

Fig. 4. Assessment of residual cellular components and quantification of osteogenic-related proteins in bone powder, DBM, and bdECM. (A) Representative images of DAPI-stained DBM and bdECM. Scale bar indicate 100 um. (B) Quantification results of DNA contents in bone powder, DBM, and bdECM ($p^* < 0.05$). Quantification results of (C) BMP-2 ($p^* < 0.05$) and (D) BMP-7 in bone powder, DBM, and bdECM ($p^* < 0.05$ compared to the bone-powder group).

investigate the contents of BMP-2 and BMP-7. If bone powder and DBM were not ground, both groups eluted much less amount of BMP-2 and BMP-7 that after grinding samples. This results might be indicated that if bone powder and the DBM is implanted *in vivo*, they are hard to lead the osteogenic effect. On the contrary, bdECM easily exposed those osteogenic related proteins on its ECM structures because it was possible to water-soluble. These facts indicated that the bdECM could be improved biological interaction with host cells by providing osteoinductive molecules and similar native physiologically relevant signal to attract cells from the implant area [11].

Effects of bone powder, DBM, and bdECM on osteogenic differentiation and mineralization in vitro

We investigated the ability to induce osteogenic differentiation using isolated primary osteoblasts with bone powder, DBM, and bdECM (Fig. 5). Our materials were put inside transwell insert and then osteoblasts were cultured at the bottom of the plate. In this experimental condition, the released factor from the materials can affect the differentiation of the osteoblasts without direct contact. We progressed to investigate calcium deposition via Von Kossa and Alizarin Red S staining after two and four weeks. Two weeks later, calcium deposition was clearly observed in the bdECM group, but no deposition or partial deposition of calcium was found in the bone powder and DBM groups (Fig. 5A). After four weeks of differentiation, overall calcium deposition trend was similar to the two- week results: bdECM exhibited better calcium deposition than did the other groups (Fig. 5B). This differentiation-inducing ability of the bdECM was re-verified by measuring the expressions of osteogenic-related genes, such as RUNX2, OCN, and OPN, after two and four weeks (Fig. 5C). The RUNX2, an early marker of osteogenic differentiation, was expressed in all experimental groups at two weeks, but no group was expressed after four weeks of differentiation, indicating that the cells on the materials were at initial differentiation status. Even though OPN expression in all groups was not significantly increased at two and four weeks, we found that the bdECM group

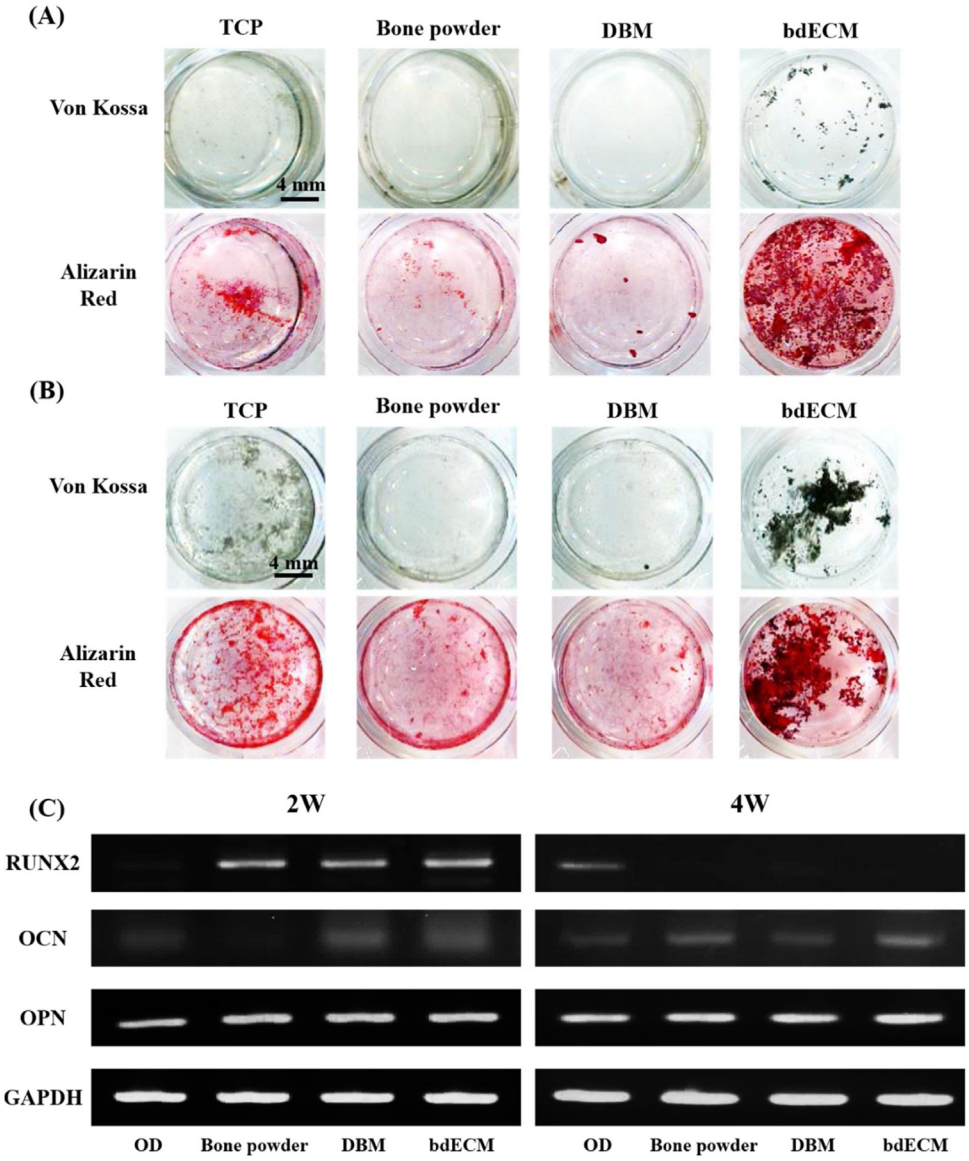

Fig. 5. *In vitro* osteogenic differentiation test on each group. Representative images of von Kossa and Alizarin Red S staining of osteoblasts cultured with bone powder, DBM, and bdECM for (A) two and (B) four weeks. (C) RT-PCR was done to investigate the osteogenic-related gene expressions of RUNX2, OCN, and OPN on bone powder, DBM, and bdECM for two and four weeks.

allowed the cell lead to the late stage of the differentiation, as compared to other groups at four weeks.

Previously, Grayson et al. demonstrated that human mesenchymal stem cells that were cultured in decellularized bovine trabecular bone scaffolds for five weeks were successfully differentiated into specific target-related tissues [30,31]. Consistent with their results, our bdECM group induced higher mineral deposition and osteogenic-related gene expressions more than did the other groups. The reasons can be deduced from the presence or exposure of BMPs in the bdECM group. Because we already measured the contents of BMPs (Fig. 4C, D), bdECM might release much more osteogenic biomolecules and improve osteogenic differentiation. Also, we supposed that cultured osteoblasts provided tissue-specific signals to differentiate into an osteogenic phenotype favorably from bdECM. These facts showed that tissue-specific ECM would play a critical role with regulated cellular differentiation.

In vivo animal test

For proving the bone-regeneration capacity of each group, we implanted the orthotopic graft as three experimental samples into the mouse calvarial defects, and examined newly formed bone volume (BV) per tissue volume (TV) and bone mineral density (BMD) (Fig. 6). We tracked newly formed bone in each group to use live micro-CT at 2, 4, 6 and 8 weeks. During the experimental period, the bone-powder group had a tendency to scan because of its mineral contents at the entire defect area (Fig. 6A). For the initial two weeks, no mineral deposition was detected in either the DBM or the bdECM group in three-dimensional (3D) images, however, a small amount of mineral contents was observed in the bdECM group in soft X-ray sagittal and transaxial images. Four weeks later, the bdECM groups promoted bone mineralization in both 3D images and soft X-ray images better than did the other groups. The bone thickness of bdECM was more significantly increased than was those from other groups, whereas the DBM group did not show any mineral deposition in the defect site during the experimental period. The quantification of BV per TV and BMD showed the defect area 8 weeks after the implantation (Fig. 6B, 6C). The bdECM group (8.21 ± 6.87 %) showed significantly higher results for newly formed BV than did the bone-powder (1.27 ± 3.84 %) or DBM (1.09 ± 0.59 %) groups. Likewise, the bdECM group ($0.71 \pm 0.18\,g/mm^3$) had significantly higher BMD than did the bone-powder ($0.12 \pm 0.50\,g/mm^3$) or DBM ($0.23 \pm 0.12\,g/mm^3$) groups. These results show that osteoinductivity of BMPs was effective in the bone-healing process.

Many researchers recently suggested that decellularized ECM derived from various tissues could promote their functions in an appropriate site by expected properties *in vivo* condition [14,32,33]. For instance, Karalashvili and colleagues implanted a decellularized, large bovine bone graft into the traumatic defect of human maxillofacial bone for reconstruction [33]. They

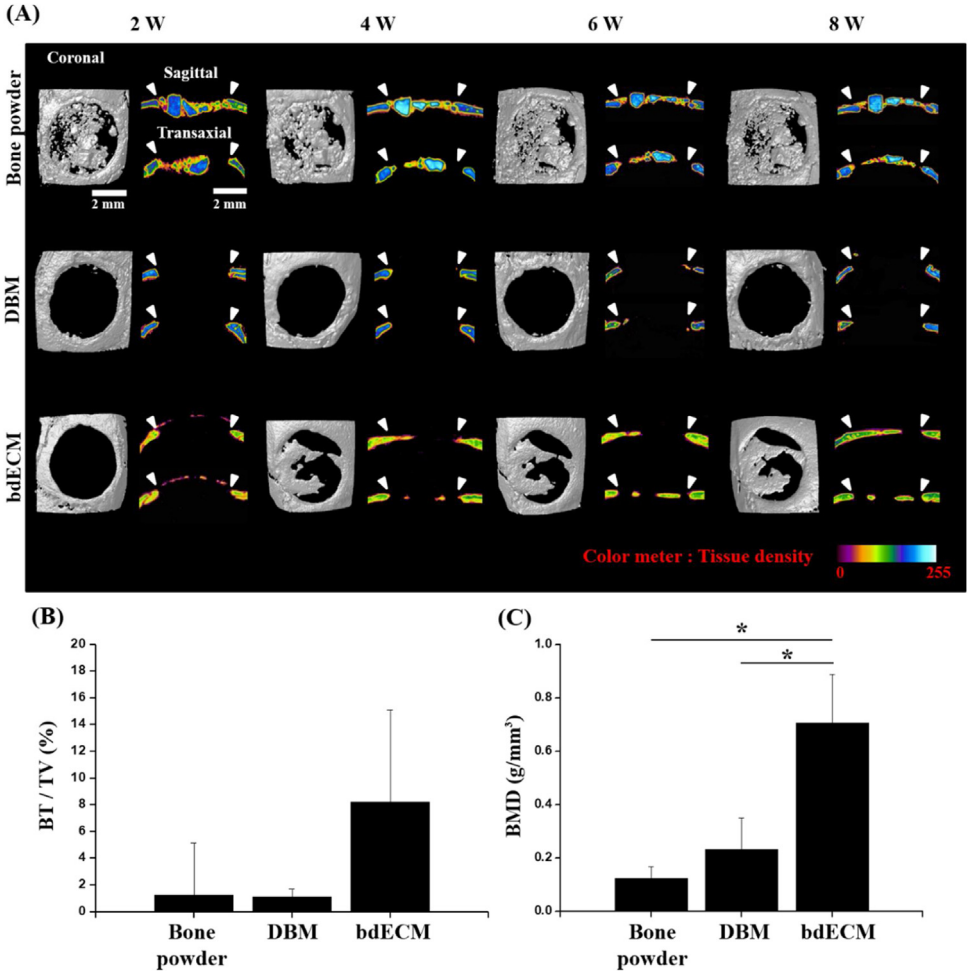

Fig. 6. Evaluation of bone regeneration in mouse calvarial defect via live micro-CT. (A) Representative live micro-CT images of bone powder, DBM, and bdECM at each time point. Arrow heads indicate the defects margin. Quantification of (B) BV/TV and (C) BMD of bone powder, DBM, and bdECM at 8 weeks ($p^* < 0.05$ compared to the bone-powder group).

demonstrated that the decellularized bovine bone graft was well-integrated with the host bone, and no complications were revealed for a year after implantation. Taken together, decellularized ECM derived from the tissues can provide specific tissue signals, which represented a binding motif and physiologically relevant and unique biochemical profiles dependent upon the derived tissues [14].

Histological and immunohistochemical analysis

We did a histological and immunohistochemical analysis to investigate more detailed histomorphological differences between these three group (Fig. 7). In H&E and Goldner's trichrome staining (Fig. 7A, B), the bone-powder group induced inflammatory responses; the implanted scaffold was surrounded by fibrotic tissues and new bone was partially integrated with the scaffold, consistent with micro-CT analysis. Additionally, the DBM-treated group had a mild immunogenic response at the defect area. As we saw in Fig. 4C and 4D, bone powder and DBM also possessed growth factors to induce bone regeneration, but these inflammatory reactions intensified the fibrosis and could be prevented signaling pathway for performing bone regeneration by host bone-forming cells. However, the bdECM group had well-integrated and newly formed bone with the host tissue, with thicker bone than from the other groups. We did not find any mild immunogenic tissues around the bdECM-implanted area. The newly formed bone area was 65.31 ± 14.87 % of the bdECM group, which was a significantly higher amount of 9.45 ± 7.97 % of bone powder and 7.16 ± 3.96 % of the DBM groups (Fig. 7C). As is consistent with the results of the bone-formation area, the bdECM group (81.18 ± 8.43 %) was observed to have better bone mineral density than did the bone-powder (1.34 ± 0.3 %) and DBM (2.32 ± 0.88 %) groups (Fig. 7D). Furthermore, the results of immunohistochemical staining with OPN, which is a very important osteogenic differentiation marker, also showed a higher positive expression in the bdECM-treated group than in the other groups (Fig. 7E).

As we have already confirmed that bdECM provided BMP-2 and BMP-7, these natural BMPs derived from bovine bone could improve new bone regeneration. [34] These growth factors can affect the recruitment of mesenchymal stem cells as well as

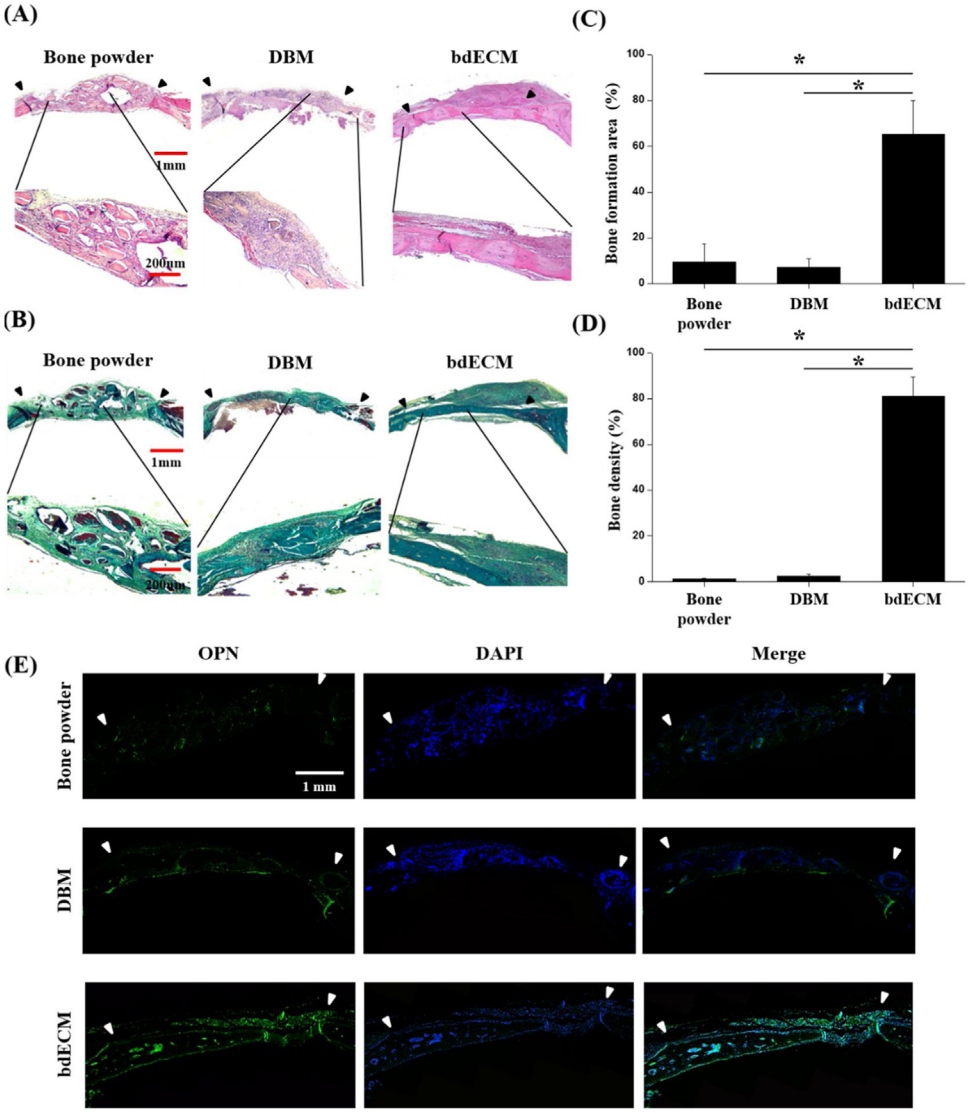

Fig. 7. Histological and immunohistochemical analysis of retrieved samples for mouse calvarial bone regeneration. Representative images of (A) H&E and (B) Goldner's trichrome staining of bone powder, DBM, and bdECM groups after eight weeks. Black arrowheads indicate the defect margin. The quantification of (C) newly formed bone formation area and (D) bond density after eight weeks ($p^* < 0.05$). (E) Representative immunofluorescence staining images of OPN and DAPI at defect sites with each group. White arrowheads indicate defect margins.

osteoblast adhesion and induction of osteogenesis at the defect site [34]. Also, these proteins activate to produce ECM proteins from osteoblasts by inhibiting metalloproteinases, which are known as regulating ECM production and degradation as a proteolytic enzyme [34,35]. For these reasons connected with our results, the effectiveness of bdECM was considered to induce positive consequences by providing the simultaneously physiological relevant signal for improving cell adhesion and growth that affected cell recruitment and differentiation better than did the other groups.

Conclusion

In the present study, we introduced a bdECM scaffold as a novel platform for effective bone regeneration. Through simple demineralization and decellularization, we have been able to manufacture the scaffold that minimizes DNA contamination and meets the minimum standards of immune response that can be used in medical applications. The bdECM had higher concentrated amounts of bone-forming bioactive molecules (BMP-2 and BMP-7) and a fibrous structure mimicking the microenvironment of native ECM. These features enabled the cells on the matrix to exhibit higher mineralization and expressions of bone-maturation-related genes. Therefore, bdECM implanted in the mouse calvarial defect model improved not only new bone formation without any further inflammatory reaction, but also mature bone regeneration during bone development. We emphasized that the bdECM is possible to provide tissue-specific physiological signals and biochemical profiles and propose that a decellularized platform including our bdECM may replace sufficiently autologous bone and DBM.

Author contributions

The manuscript was written through equal contribution of Min Suk Lee and Dong Hyun Lee.

Note

The authors declare no competing financial interest.

Declaration of interests

The authors declare that they have no known competing financial interests or personal relationships that could have appeared to influence the work reported in this paper.

Acknowledgments

This work was supported by the National Research Foundation of Korea (NRF) grant funded by the Korea government (MSIP) (NRF-2018R1A4A1024963). Also, the authors gratefully acknowledge Center for Bio-Medical Engineering Core Facility at Dankook University for providing critical reagents and equipment.

References

1 K. Chen, X. Lin, Q. Zhang, J. Ni, J. Li, J. Xiao, et al., Acta Biomater. 19 (2015) 46–55.
2 X. Gao, J. Song, Y. Zhang, X. Xu, S. Zhang, P. Ji, et al., ACS Appl. Mater. Interfaces (2016).
3 M.P. Ginebra, T. Traykova, J.A. Planell, J Controlled Release 113 (2006) 102–110.
4 M.J. Sawkins, W. Bowen, P. Dhadda, H. Markides, L.E. Sidney, A.J. Taylor, et al., Acta Biomater. 9 (2013) 7865–7873.
5 J. Shi, J. Sun, W. Zhang, H. Liang, Q. Shi, X. Li, et al., ACS Appl. Mater. Interfaces (2016).
6 B. Peterson, P.G. Whang, R. Iglesias, J.C. Wang, J.R. Lieberman, J. Bone Joint Surg. Am. 86-A (2004) 2243–2250.
7 J.C. Wang, A. Alanay, D. Mark, L.E. Kanim, P.A. Campbell, E.G. Dawson, et al., Eur. Spine J. 16 (2007) 1233–1240.
8 E. Gruskin, B.A. Doll, F.W. Futrell, J.P. Schmitz, J.O. Hollinger, Adv. Drug Deliv. Rev. 64 (2012) 1063–1077.
9 M.P. Bostrom, X. Yang, M. Kennan, H. Sandhu, E. Dicarlo, J.M. Lane, Spine 26 (2001) 1425–1428.
10 D.C. Markel, S.T. Guthrie, B. Wu, Z. Song, P.H. Wooley, J. Inflamm. Res. 5 (2012) 13–18.
11 K.E. Benders, P.R. van Weeren, S.F. Badylak, D.B. Saris, W.J. Dhert, J. Malda, Trends Biotech. 31 (2013) 169–176.
12 F. Pati, T.H. Song, G. Rijal, J. Jang, S.W. Kim, D.W. Cho, Biomaterials 37 (2015) 230–241.
13 J.Y. Kim, G. Ahn, C. Kim, J.S. Lee, I.G. Lee, S.H. An, et al., Macromol. Biosci. 18 (2018)e1800025.
14 T.L. Sellaro, A. Ranade, D.M. Faulk, G.P. McCabe, K. Dorko, S.F. Badylak, et al., Tissue Eng. Part A 16 (2010) 1075–1082.
15 J. Wu, Q. Ding, A. Dutta, Y. Wang, Y.H. Huang, H. Weng, et al., Acta Biomater. 16 (2015) 49–59.
16 T.W. Gilbert, J.M. Freund, S.F. Badylak, J. Surg Res. 152 (2009) 135–139.
17 T.J. Keane, R. Londono, N.J. Turner, S.F. Badylak, Biomaterials 33 (2012) 1771–1781.
18 X. Ding, X. Wei, Y. Huang, C. Guan, T. Zou, S. Wang, et al., J. Mat. Chem. B 3 (2015) 3177–3188.
19 J.F. Kirk, G. Ritter, C. Waters, S. Narisawa, J.L. Millan, J.D. Talton, Cell Tissue Bank. 14 (2013) 33–44.
20 M. Janko, J. Sahm, A. Schaible, J.C. Brune, M. Bellen, K. Schroder, et al., J. Tissue Eng. Regen. Med. 12 (2018) 653.
21 M.A. Soicher, B.A. Christiansen, S.M. Stover, J.K. Leach, D.P. Fyhrie, J. Mech Behav. Biomed. Mat. 26 (2013) 109.
22 M.K. Herliansyah, M. Hamdi, A. Ide-Ektessabi, M.W. Wildan, J.A. Toque, Mat. Sci. Eng. C 29 (2009) 1674.
23 P.M. Crapo, T.W. Gilbert, S.F. Badylak, Biomaterials 32 (2011) 3233.
24 J.E. Reing, B.N. Brown, K.A. Daly, J.M. Freund, T.W. Gilbert, S.X. Hsiong, et al., Biomaterials 31 (2010) 8626.
25 R. Yoshida, P. Vavken, M.M. Murray, Knee 19 (2012) 672.
26 M.J. Eagle, P. Rooney, J.N. Kearney, Cell Tissue Bank. 16 (2015) 433.
27 F.S.R. Carvalho, V.P. Feitosa, P.G.B. Silva, E.C.S. Soares, T.R. Ribeiro, C.S.R. Fonteles, et al., J. Cranio-maxillo-facial Surg. 46 (2018) 749.
28 A.M. Matuska, M.F. Dolwick, P.S. McFetridge, J. Mat Sci. 29 (2018) 152.
29 Z.E. Pflum, S.L. Palumbo, W.J. Li, Experimental Cell Res. 319 (2013) 1942.
30 W.L. Grayson, M. Frohlich, K. Yeager, S. Bhumiratana, M.E. Chan, C. Cannizzaro, et al., Proc. Natl. Acad. Sci. U.S.A 107 (2010) 3299.
31 C.W. Cheng, L.D. Solorio, E. Alsberg, Biotechnol Adv 32 (2014) 462.
32 B.E. Uygun, A. Soto-Gutierrez, H. Yagi, M.L. Izamis, M.A. Guzzardi, C. Shulman, et al., Nature Med. 16 (2010) 814.
33 L. Karalashvili, N. Chichua, G. Menabde, L. Atskvereli, T. Grdzelidze, A. Machavariani, M. Zurmukhtashvili, K. Gogilashvili, Z. Kakabadze, Z. Chichua, Medical Case Rep. 04 (2018).
34 C. Laflamme, M. Rouabhia, Biomed. Mat. 3 (2008)015008.
35 M.D. Sternlicht, Z. Werb, Ann. Rev. Cell Dev. Biol. 17 (2001) 463.